*Progress In Electromagnetics Research B, Vol. 24, 241–262, 2010*

# AVERAGE INTENSITY AND SPREADING OF PARTIALLY COHERENT FOUR-PETAL GAUSSIAN BEAMS IN TURBULENT ATMOSPHERE

**J. Li, Y. Chen, S. Xu, Y. Wang, M. Zhou, Q. Zhao, Y. Xin and F. Chen**

Department of Optical Engineering
Nanjing University of Science and Technology
Nanjing, Jiangsu 210094, China

**Abstract**—The concept of partially coherent four-petal Gaussian (PCFPG) beam is introduced and described in analytical forms. Based on the Huygens-Fresnel integral formula, average intensity and beam spreading in turbulent atmosphere are derived in analytical expressions. Effects of beam parameters and atmospheric structure constant on intensity distributions and effective beam sizes are investigated in detail, respectively. Results show that PCFPG beams carrying larger coherence lengths or higher beam orders would be less affected by turbulence. It is also indicated that, when the propagation distance increases, the PCFPG beam would convert into the Gauss-like profile sooner or later, but this degradation can be reduced by modulating beam parameters. Results in this paper may provide potential applications in free-space optical communications.

## 1. INTRODUCTION

In recent years, the propagation of various laser beams in turbulent atmosphere has become a hotspot in the theory of atmospheric optics, and it has attracted much interest of researchers due to its essential applications in free-space optical communications [1–3] and remote sensing [4–6] etc. A great many investigations have been made on propagation properties of various laser beams in turbulent atmosphere [7–30]. Many influential analytical methods are carried out to overcome the turbulence-induced degradation [2, 3, 20, 28, 31–33]. It has been widely recognized that partially coherent

*Received 23 June 2010, Accepted 11 August 2010, Scheduled 16 August 2010*
Corresponding author: J. Li (lijiafeifei@sina.com).

laser beams are less affected by turbulence than their coherent counterparts [7, 18, 24, 29, 32]. It is also indicated that the use of higher-order model source can also reduce this degradation [3, 27, 28]. Based on above two results, a trend can be estimated that, in near future, it is necessary and essential to study propagation properties of partially coherent higher-order model beams in turbulent atmosphere, in order to further overcome the degradation caused by turbulent atmosphere.

On the other hand, recently beam pattern formations and beam shaping have attracted more and more attentions as well as their propagation properties [34–42]. Since then, methods of generating various beam patterns have found wide applications in optical resonators [43, 44]. Very recently, a new form of laser beams called the four-petal Gaussian (FPG) beam is introduced in analytical expressions [45], and subsequently its propagation properties in various media are investigated in detail [46–52]. Although these works are valuable and significant, to our knowledge, they have not taken into account the partially coherent case. Also strictly speaking, fully coherent laser beams are not existing in practice.

According to the two unsettled issue stated above, in this paper, a partially coherent four-petal Gaussian (PCFPG) beam is introduced, and its propagation properties in turbulent atmosphere are derived in analytical expressions. By numerical examples, effects of beam parameters and atmospheric structure constant on average intensity and beam spreading are studied, respectively.

## 2. PROPAGATION THEORY

In the Cartesian coordinate system, the electric field of a coherent four-petal Gaussian (FPG) beam in the initial plane $z = 0$ is given by [45–53]

$$E_n\left(x, y; 0\right) = \left(\frac{xy}{\sigma_0^2}\right)^{2n} \exp\left(-\frac{x^2+y^2}{\sigma_0^2}\right), \quad n = 0, 1, 2\ldots, \qquad (1)$$

where $n$ is the order of the four-petal Gaussian beam, $\sigma_0$ is the waist width of fundamental Gaussian beams. When $n = 0$, Eq. (1) reduces to the expression of fundamental Gaussian beams. In Eq. (1), the time variation factor $\exp(-i\omega t)$ is omitted. Detailed behaviors of four-petal Gaussian beams in the initial plane have been investigated in [45]. In this paper, the existing coherent FPG beam is extended to a partially coherent case, and the cross-spectral density of latter can be represented as [53]

$$\begin{aligned} W\left(x_1, y_1, x_2, y_2; 0\right) &= \left\langle E_n^*\left(x_1, y_1; 0\right) E_n\left(x_2, y_2; 0\right)\right\rangle \\ &= \sqrt{I\left(x_1, y_1; 0\right) I\left(x_2, y_2; 0\right)}\mu\left(x_1 - x_2, y_1 - y_2; 0\right), \quad (2) \end{aligned}$$

where $I(x, y; 0) = W(x, y, x, y; 0)$ is the intensity at the initial plane by evaluating $x_1 = x_2 = x$ and $y_1 = y_2 = y$ of the cross-spectral density; $\mu(x_1 - x_2, y_1 - y_2; 0)$ is the spectral degree of coherence assumed to have the Gaussian profile

$$\mu\left(x_1 - x_2, y_1 - y_2; 0\right) = \exp\left[-\frac{\left(x_1 - x_2\right)^2 + \left(y_1 - y_2\right)^2}{2\delta_g^2}\right], \quad (3)$$

where $\delta_g$ is defined as the transversal coherence length of the PCFPG source beam. Substituting Eq. (1) and Eq. (3) into Eq. (2), the cross-spectral density of PCFPG beams in the initial plane can be expressed as

$$\begin{aligned} W\left(x_1, y_1, x_2, y_2; 0\right) &= \left(\frac{x_1 y_1}{\sigma_0^2}\right)^{2n} \left(\frac{x_2 y_2}{\sigma_0^2}\right)^{2n} \exp\left(-\frac{x_1^2 + y_1^2 + x_2^2 + y_2^2}{\sigma_0^2}\right) \\ &\times \exp\left[-\frac{\left(x_1 - x_2\right)^2 + \left(y_1 - y_2\right)^2}{2\delta_g^2}\right], \quad (4) \end{aligned}$$

when $n = 0$, Eq. (4) reduces to the cross-spectral density of partially coherent Gaussian Schell-model beams [7].

Under the paraxial approximation, the propagation of laser beams in turbulent atmosphere can be treated with the extended Huygens-Fresnel integral formula, of which the average intensity in the output plane $z$ can be given by [24, 28, 30]

$$\begin{aligned} \left\langle I\left(p, q; z\right)\right\rangle = & \frac{k^2}{4\pi^2 z^2} \int_{-\infty}^{+\infty} \int_{-\infty}^{+\infty} \int_{-\infty}^{+\infty} \int_{-\infty}^{+\infty} W\left(x_1, y_1, x_2, y_2; 0\right) \\ & \exp\left[-\frac{ik}{2z}\left(x_1 - p\right)^2 - \frac{ik}{2z}\left(y_1 - q\right)^2\right] \\ & \times \exp\left[\frac{ik}{2z}\left(x_2 - p\right)^2 + \frac{ik}{2z}\left(y_2 - q\right)^2\right] \\ & \left\langle \exp\left[\psi^*\left(x_1, y_1\right) + \psi\left(x_2, y_2\right)\right]\right\rangle dx_1 dx_2 dy_1 dy_2, \quad (5) \end{aligned}$$

where the angle brackets denotes the ensemble average over the turbulence, and the asterisk denotes the complex conjugation, $k$ is the wave number which is related to the wavelength $\lambda$ as $k = 2\pi/\lambda$. The ensemble average in Eq. (5) can be approximately represented in the Rytov's phase function [25–27]

$$\begin{aligned}\langle \exp\left[\psi^*\left(x_1,y_1\right)+\psi\left(x_2,y_2\right)\right]\rangle &= \exp\left[-0.5D_\psi\left(x_1-x_2,y_1-y_2\right)\right]\\ &= \exp\left[-\frac{\left(x_1-x_2\right)^2+\left(y_1-y_2\right)^2}{\rho_0^2}\right], \quad (6)\end{aligned}$$

where $D_\psi$ is the wave structure function which is approximated by the phase structure function in Rytov's representations [20–28, 54], $\rho_0 = \left(0.545C_n^2k^2z\right)^{-3/5}$ is the spherical wave coherence length, $C_n^2$ is the structure constant of local turbulent atmosphere. Substituting Eq. (4) and Eq. (6) into Eq. (5) and making use of the integral transform technique, after tedious integral calculations (see Appendix A), the average intensity distributions in the output plane $z$ can be obtained as

$$\begin{aligned}\langle I\left(p,q;z\right)\rangle &= \frac{k^2\left[(2n)!\right]^4}{4z^2\cdot 2^{12n}}\frac{1}{\sqrt{R_S^+R_Q^+}}\\
&\exp\left\{-\frac{k^2p^2}{4R_Q^+z^2}\left[\frac{1}{2R_S^+}\left(\frac{1}{\delta_g^2}+\frac{2}{\rho_0^2}\right)-1\right]^2-\frac{k^2p^2}{4R_S^+z^2}\right\}\\
&\times\exp\left\{\frac{k^2q^2}{4R_Q^+z^2}\left[\frac{1}{2R_S^+}\left(\frac{1}{\delta_g^2}+\frac{2}{\rho_0^2}\right)-1\right]^2-\frac{k^2q^2}{4R_S^+z^2}\right\}\\
&\sum_{s=0}^{n}\sum_{t=0}^{n}\sum_{h=0}^{n}\sum_{l=0}^{n}\frac{1}{(n-s)!\,(2s)!\,(n-t)!\,(2t)!}\\
&\times\frac{1}{(n-h)!\,(2h)!\,(n-l)!\,(2l)!}\sum_{f=0}^{2s}\sum_{g=0}^{2t}\binom{2s}{f}\binom{2t}{g}\\
&\sum_{u=0}^{[f/2]}\sum_{v=0}^{h}\sum_{r=0}^{[g/2]}\sum_{d=0}^{l}\frac{f!\,(2h)!}{u!\,(f-2u)!v!\,(2h-2v)!}\\
&\times\frac{g!\,(2l)!}{r!\,(g-2r)!d!\,(2l-2d)!}(-1)^{u+v+r+d}\left(\frac{1}{2}-\frac{1}{R_S^+\sigma_0^2}\right)^{s+t}\\
&(2i)^{2u+2v+2r+2d-f-2h-g-2l}\left(\frac{8}{\sigma_0^2}\right)^{h+l-r-d}\\
&\times\left(\frac{1}{\sqrt{R_Q^+}}\right)^{f+g+2h+2l-2u-2v-2r-2d}\end{aligned}$$

$$\left(\frac{\frac{2}{\delta_g^2}+\frac{4}{\rho_0^2}}{\sqrt{{R_S^+}^2\sigma_0^2-2R_S^+}}\right)^{f+g-2u-2v} H_{2s-f}\left(\frac{ikp}{\sqrt{{R_S^+}^2\sigma_0^2-2R_S^+z}}\right)$$
$$\times H_{2t-g}\left(\frac{ikq}{\sqrt{{R_S^+}^2\sigma_0^2-2R_S^+z}}\right)H_{f+2h-2u-2v}$$
$$\left\{-\frac{kp}{2\sqrt{R_Q^+}z}\left[\frac{1}{2R_S^+}\left(\frac{1}{\delta_g^2}+\frac{2}{\rho_0^2}\right)-1\right]\right\}$$
$$\times H_{g+2l-2r-2d}\left\{-\frac{kq}{2\sqrt{R_Q^+}z}\left[\frac{1}{2R_S^+}\left(\frac{1}{\delta_g^2}+\frac{2}{\rho_0^2}\right)-1\right]\right\}, \tag{7}$$

where $H_n(.)$ is the Hermite polynomial of order $n$, and factors $R_S^+, R_Q^+$ are represented by

$$R_S^+=\frac{1}{\sigma_0^2}+\frac{1}{2\delta_g^2}+\frac{1}{\rho_0^2}+\frac{ik}{2z},\quad R_Q^+=\frac{1}{R_S^+}\left(\frac{1}{\sigma_0^2\delta_g^2}+\frac{1}{\sigma_0^2}+\frac{2}{\sigma_0^2\rho_0^2}+\frac{k^2}{4z^2}\right), \tag{8}$$

Equation (7) is the analytical formula for average intensity distributions of a partially coherent four-petal Gaussian beam in turbulent atmosphere, and it can provide a convenient way to study turbulence-induced degradations in a detailed fashion.

Now let us discuss some special cases of Eq. (7). When $n = 0$, Eq. (7) reduces to the expression for average intensity distributions of Gaussian Schell-model beams in turbulent atmosphere [7, 21]

$$\langle I_{GSM}(p,q;z)\rangle = \left(\frac{k}{2z}\right)^2\frac{1}{\tilde{R}_S+\tilde{R}_S^-}\exp\left\{-\frac{k^2p^2}{4\tilde{R}_S^-z^2}-\frac{k^2q^2}{4\tilde{R}_S^-z^2}\right\}$$
$$\exp\left\{-\frac{k^2}{4\tilde{R}_S+z^2}\left(p^2+q^2\right)\right\}, \tag{9}$$

where $\tilde{R}_S+, \tilde{R}_S^-$ are respectively given by

$$\tilde{R}_S+=\frac{1}{\sigma_0^2}+\frac{1}{2\delta_g^2}+\frac{1}{\rho_0^2}+\frac{ik}{2z},\quad \tilde{R}_S^-=\frac{1}{\sigma_0^2}+\frac{1}{2\delta_g^2}-\frac{1}{4\tilde{R}_S+\delta_g^4}-\frac{ik}{2z}, \tag{10}$$

when $\delta_g\to\infty$ is satisfied, Eq. (7) can be rewritten to Eq. (8) of [47], which corresponds to the expression for average intensity distributions of coherent FPG beams in turbulent atmosphere. When $C_n^2 = 0$, Eq. (7) reduces to the propagation formula for PCFPG beams in free space [55].

The effective beam sizes of PCFPG beams in the $x$ and $y$ directions in the output plane can be defined by using moments of two orders of $x$ and $y$ variance [25, 30, 56]

$$W_j(z) = \sqrt{\frac{2\int j^2 \langle I(p,q;z)\rangle dpdq}{\int \langle I(p,q;z)\rangle dpdq}}, \quad (j = p, q) \tag{11}$$

substituting Eqs. (4)–(6) into Eq. (11) and inverting the integration order, after tedious integrations (see Appendix A), the analytical effective beam sizes of PCFPG beams yield

$$W_p = W_q = \sqrt{\frac{2J_1(z)}{J_2(z)}}, \tag{12}$$

where $J_1(z)$ and $J_2(z)$ are respectively given by

$$J_1(z) = \frac{\pi k^2 [(2n)!]^4}{4z^2 \cdot 2^{12n}} \frac{1}{\sqrt{R_S^+ R_Q^+}}$$
$$\sum_{s=0}^{n}\sum_{t=0}^{n}\sum_{h=0}^{n}\sum_{l=0}^{n} \frac{1}{(n-s)!(2s)!(n-t)!(2t)!(n-h)!(2h)!(n-l)!(2l)!}$$
$$\times \sum_{f=0}^{2s}\sum_{g=0}^{2t} \binom{2s}{f}\binom{2t}{g} \sum_{u=0}^{[f/2]}\sum_{v=0}^{h}\sum_{r=0}^{[g/2]}\sum_{d=0}^{l}$$
$$(2s-f)!(2t-g)!(f+2h-2u-2v)!(g+2l-2r-2d)!$$
$$\times \sum_{a_1=0}^{[(2s-f)/2]} \sum_{a_2=0}^{[(2t-g)/2]} \sum_{b_1=0}^{[(f+2h-2u-2v)/2]} \sum_{b_2=0}^{[(g+2l-2r-2d)/2]}$$
$$\frac{1}{a_1!(2s-f-2a_1)!a_2!(2t-g-2a_2)!}$$
$$\times \frac{1}{b_1!(f+2h-2u-2v-2b_1)!b_2!(g+2l-2r-2d-2b_2)!}$$
$$(-1)^{u+v+r+d+a_1+b_1+a_2+b_2}$$
$$\times (2i)^{4u+4v+4r+4d+2b_1+2b_2-4h-4l-2f-2g-2}$$
$$\left(\frac{1}{\sqrt{R_Q^+}}\right)^{f+g+2h+2l-2u-2v-2r-2d} \left(\frac{8}{\sigma_0^2}\right)^{h+l-r-d}$$
$$\times\left(\frac{\frac{2}{\delta_g^2}+\frac{4}{\rho_0^2}}{\sqrt{{R_S^+}^2\sigma_0^2-2R_S^+}}\right)^{f+g-2u-2v}\left(\frac{k}{\sqrt{{R_S^+}^2\sigma_0^2-2R_S^+}}\right)^{2s+2t-f-g-2a_1-2a_2}$$

$$\times\left\{\frac{k^2}{4R_S^+z^2}+\frac{k^2}{4R_Q^+z^2}\right.$$

$$\left.\left[\frac{1}{2R_S^+}\left(\frac{1}{\delta_g^2}+\frac{2}{\rho_0^2}\right)-1\right]^2\right\}^{u+v+r+d+a_1+b_1+a_2+b_2-s-t-h-l-2}$$

$$\times\left\{-\frac{k}{\sqrt{R_Q^+}z}\left[\frac{1}{2R_S^+}\left(\frac{1}{\delta_g^2}+\frac{2}{\rho_0^2}\right)-1\right]\right\}^{f+g+2h+2l-2u-2v-2r-2d-2b_1-2b_2}$$

$$\times H_{2s+2h-2u-2v-2a_1-2b_1}(0)\,H_{2t+2l-2r-2d-2a_2-2b_2+2}(0), \tag{13}$$

$$J_2(z)=\frac{\pi k^2\left[(2n)!\right]^4}{4z^2\cdot 2^{12n}}\frac{1}{\sqrt{R_S^+R_Q^+}}$$

$$\sum_{s=0}^{n}\sum_{t=0}^{n}\sum_{h=0}^{n}\sum_{l=0}^{n}\frac{1}{(n-s)!\,(2s)!\,(n-t)!\,(2t)!\,(n-h)!\,(2h)!\,(n-l)!\,(2l)!}$$

$$\times\sum_{f=0}^{2s}\sum_{g=0}^{2t}\binom{2s}{f}\binom{2t}{g}\sum_{u=0}^{[f/2]}\sum_{v=0}^{h}\sum_{r=0}^{[g/2]}\sum_{d=0}^{l}$$

$$(2s-f)!\,(2t-g)!\,(f+2h-2u-2v)!\,(g+2l-2r-2d)!$$

$$\times\sum_{a_1=0}^{[(2s-f)/2]}\sum_{a_2=0}^{[(2t-g)/2]}\sum_{b_1=0}^{[(f+2h-2u-2v)/2]}\sum_{b_2=0}^{[(g+2l-2r-2d)/2]}$$

$$\frac{1}{a_1!\,(2s-f-2a_1)!a_2!\,(2t-g-2a_2)!}$$

$$\times\frac{1}{b_1!\,(f+2h-2u-2v-2b_1)!b_2!\,(g+2l-2r-2d-2b_2)!}$$

$$(-1)^{u+v+r+d+a_1+b_1+a_2+b_2}$$

$$\times(2i)^{4u+4v+4r+4d+2b_1+2b_2-4h-4l-2f-2g}$$

$$\left(\frac{1}{\sqrt{R_Q^+}}\right)^{f+g+2h+2l-2u-2v-2r-2d}\left(\frac{8}{\sigma_0^2}\right)^{h+l-r-d}$$

$$\times\left(\frac{\frac{2}{\delta_g^2}+\frac{4}{\rho_0^2}}{\sqrt{{R_S^+}^2\sigma_0^2-2R_S^+}}\right)^{f+g-2u-2v}\left(\frac{k}{\sqrt{{R_S^+}^2\sigma_0^2-2R_S^+}}\right)^{2s+2t-f-g-2a_1-2a_2}$$

$$\times\left\{\frac{k^2}{4R_S+z^2}+\frac{k^2}{4R_Q^+z^2}\right.$$
$$\left.\left[\frac{1}{2R_S^+}\left(\frac{1}{\delta_g^2}+\frac{2}{\rho_0^2}\right)-1\right]^2\right\}^{u+v+r+d+a_1+b_1+a_2+b_2-s-t-h-l}$$
$$\times\left\{-\frac{k}{\sqrt{R_Q^+}z}\left[\frac{1}{2R_S^+}\left(\frac{1}{\delta_g^2}+\frac{2}{\rho_0^2}\right)-1\right]\right\}^{f+g+2h+2l-2u-2v-2r-2d-2b_1-2b_2}$$
$$\times H_{2s+2h-2u-2v-2a_1-2b_1}(0)\,H_{2t+2l-2r-2d-2a_2-2b_2}(0)\,, \qquad (14)$$

where $[n]$ gives the greatest integer which is less than or equal to $n$. Eq. (7) and Eqs. (13)–(14) are the main results of this paper, which allow one to investigate the average intensity and beam spreading of PCFPG beams in turbulent atmosphere. Although these derived expressions seem rather complicated in forms, which involve exponent functions, sums of binomial coefficients and Hermite polynomial etc., it only takes several minutes to run the computation by using Matlab. On the contrary it would cost several hours or even days to perform numerical integrations of Eq. (5) due to the fact that it involves four inseparable integrals.

## 3. NUMERICAL EXAMPLES AND ANALYSIS

Based on the derived analytical results in the above section, here the average intensity distributions and spreading characteristics of PCFPG beams in turbulent atmosphere are investigated by using Eq. (7) and Eqs. (13)–(14), respectively. For numerical examples, uniform beam parameters are chosen $\lambda = 632.8\,\text{nm}$, $\sigma_0 = 10\,\text{mm}$, unless otherwise stated. The normalized intensity distribution of the PCFPG beam is utilized and shown in Figs. 1–4, which is defined by the following formula [9, 17, 25, 54]

$$\left\langle \bar{I}(p,q,z)\right\rangle = \left\langle I(p,q,z)\right\rangle / \left\langle I(p,q,z)\right\rangle_{\max}\,, \qquad (15)$$

where $\langle I(p,q,z)\rangle_{\max}$ is the maximum value of the average intensity distribution $\langle I(p,q,z)\rangle$.

Figure 1 shows the 3-D normalized intensity distributions of PCFPG beams at several propagation distances in turbulent atmosphere, with $n = 1$, $C_n^2 = 10^{-14}\,\text{m}^{-2/3}$. From four subfigures, it can be seen that, when the propagation distance $z$ increases, initial four-petals gradually superpose and the beam profile correspondingly changes. When $z$ is large enough, i.e., $z = 3\,\text{km}$ in subfigure (d), beam

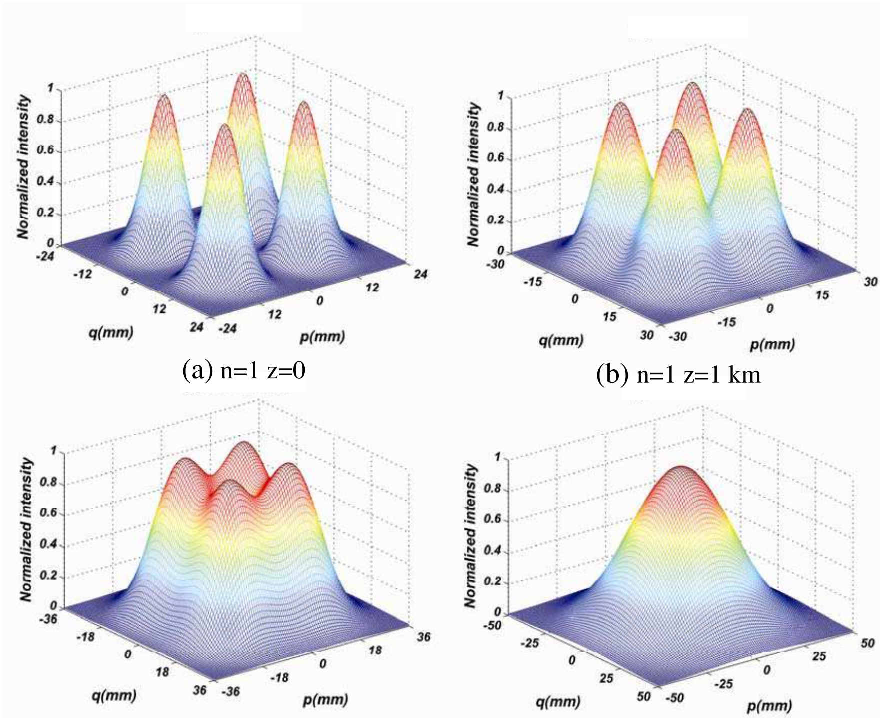


(a) n=1 z=0

(b) n=1 z=1 km

(c) n=1 z=2 km

(d) n=1 z=3 km

**Figure 1.** Normalized intensity distributions of PCFPG beams with $n = 1$ at several propagation distances in turbulent atmosphere, $\delta_g$=5 mm, $C_n^2 = 10^{-14}\,\mathrm{m}^{-2/3}$. (a) $z = 0$. (b) $z = 1\,\mathrm{km}$. (c) $z = 2\,\mathrm{km}$. (d) $z = 3\,\mathrm{km}$.

profile finally is converted to Gauss-like type. This phenomenon has been discussed in previous references [1, 7, 21, 22].

Figure 2 shows the 3-D normalized intensity distributions of PCFPG beams in turbulent atmosphere, with $n = 3$, $C_n^2 = 10^{-14}\,\mathrm{m}^{-2/3}$. Comparing to Fig. 1, it can be found that the PCFPG beam carrying higher beam order $n$ would better preserve its initial profile upon propagation in turbulent atmosphere. This result well corresponds to the existing deduction [25, 27, 28] that coherent combination beams or higher order laser beams are less influenced by turbulence than single model beams. In this paper, this deduction also holds true for the propagation of higher order PCFPG beams in turbulent atmosphere.

Figure 3 shows effects of atmospheric structure constant $C_n^2$ on

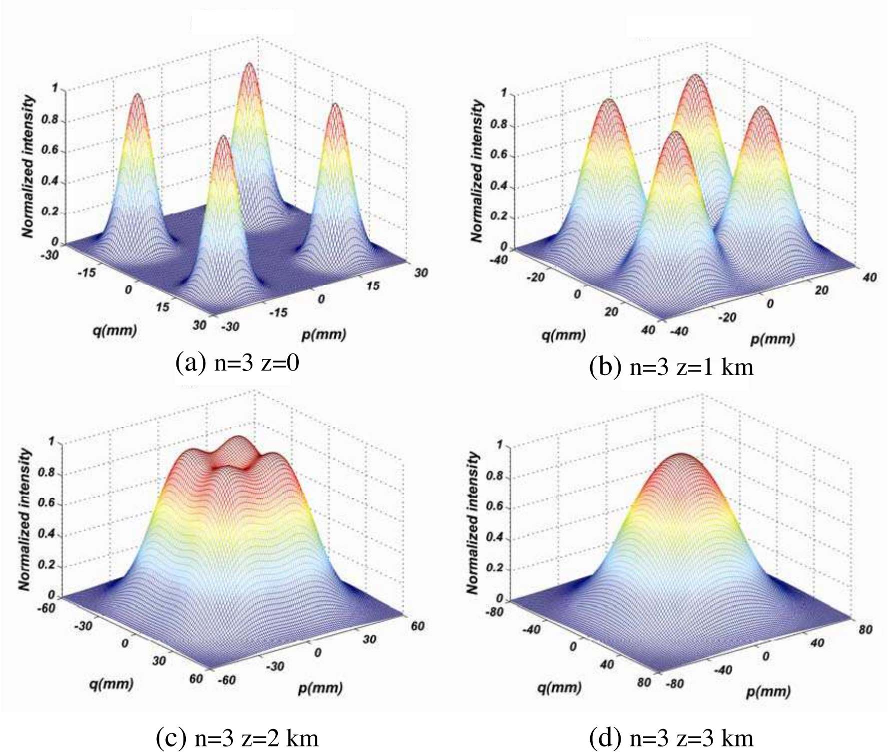


**Figure 2.** Normalized intensity distributions of PCFPG beams with $n = 3$ at several propagation distances in turbulent atmosphere, $\delta_g = 5\,\text{mm}$, $C_n^2 = 10^{-14}\,\text{m}^{-2/3}$. (a) $z = 0$. (b) $z = 1\,\text{km}$. (c) $z = 2\,\text{km}$. (d) $z = 3\,\text{km}$.

normalized transversal intensity distributions versus the slant axis. For comparisons, free space intensity distributions ($C_n^2 = 0$) are also plotted in Figs. 3(a)–(d). In subfigures (a)–(d), the slant axis is selected as the diagonal line of the Cartesian coordinate system, and other parameters are chosen $\delta_g = 5\,\text{mm}$, $n = 5$. From subfigures (a) and (b) it is indicated that, when propagation distance $z$ is not so large ($z \leq 1\,\text{km}$), atmospheric turbulence hardly affects intensity distributions of PCFPG beams, of which the reason can be explained by theories of the Rayleigh range [57]. As propagation distances subsequently increase, influence of turbulence starts to enhance. One conclusion can be made from these curves is that, with larger atmospheric structure constant, PCFPG beams would convert into the Gauss-like profile much more rapidly [see Fig. 3(d)].

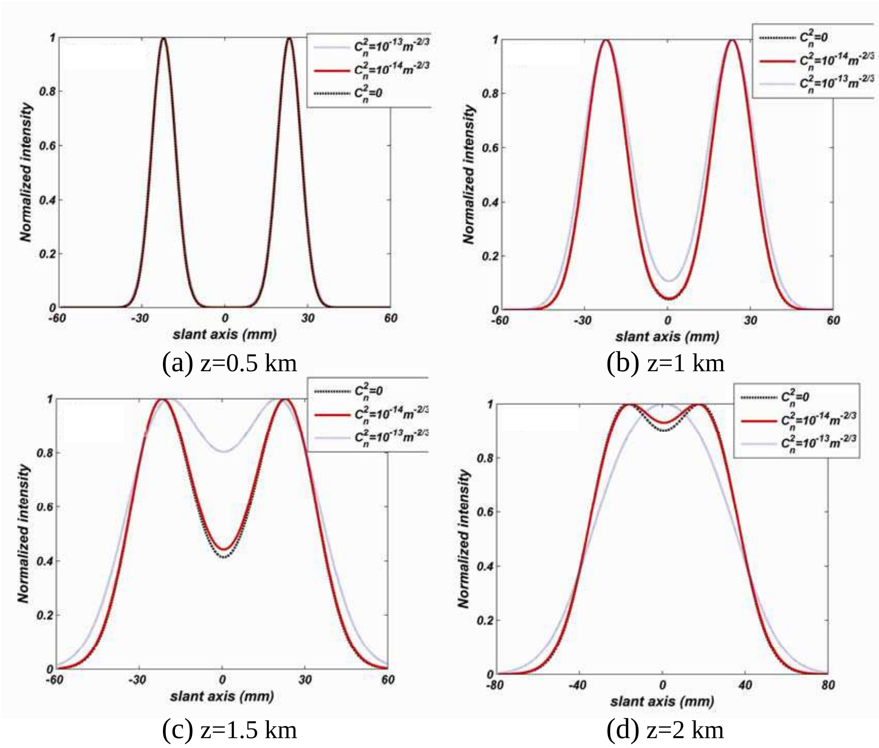


**Figure 3.** Normalized transversal intensity distributions of PCFPG beams versus slant axis for different structure constant $C_n^2$ in turbulent atmosphere, $\delta_g = 5\,\text{mm}$, $n = 5$. (a) $z = 0.5\,\text{km}$. (b) $z = 1\,\text{km}$. (c) $z = 1.5\,\text{km}$. (d) $z = 2\,\text{km}$.

Figure 4 represents effects of source coherence length $\delta_g$ on normalized transversal intensity distributions versus slant axis. For comparisons, the fully coherent case ($\delta_g$ = infinity) is also plotted in Figs. 4(a)–(d). From subfigures (a)–(d) it can be seen that in the initial plane, coherence length has no impact on intensity distributions, of which the reason can be explained by Eq. (4). However, effects of coherence length become evident when the propagation distance $z$ increases; on the other hand, with smaller coherence length of sources, PCFPG beams would convert into the Gauss-like profile much more rapidly, and this phenomenon can be observed in Fig. 4(d). Besides these, another phenomenon can be observed is that intensity distributions of off-axial reference points are less affected by coherence length than those of on-axial points.

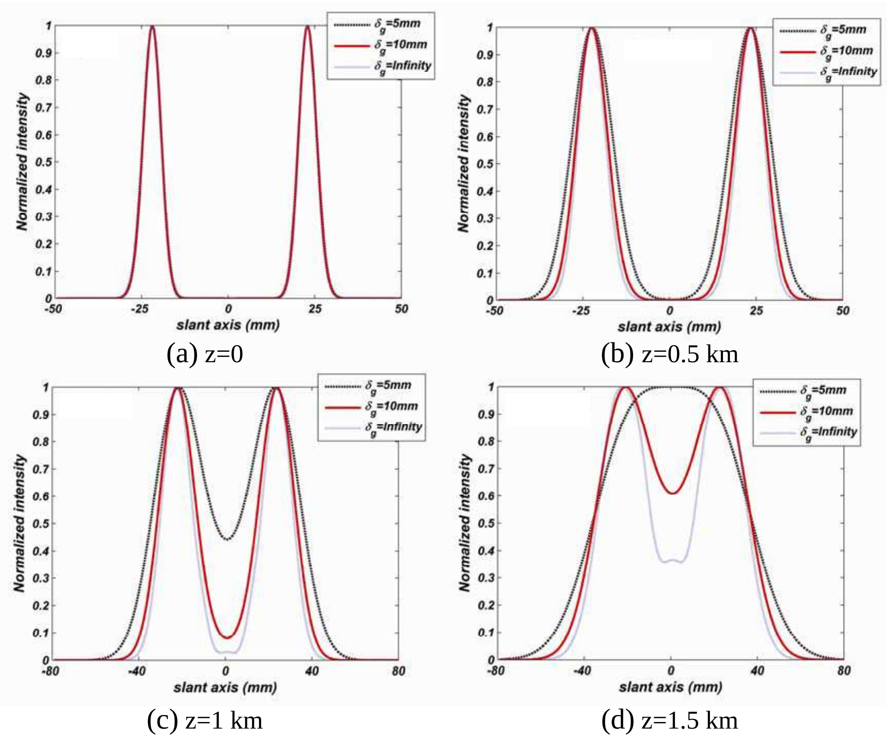


**Figure 4.** Normalized transversal intensity distributions of PCFPG beams versus slant axis for different coherence length $\delta_g$ in turbulent atmosphere, $C_n^2 = 10^{-14}\,\mathrm{m}^{-2/3}$, $n = 5$. (a) $z = 0$. (b) $z = 0.5\,\mathrm{km}$. (c) $z = 1\,\mathrm{km}$. (d) $z = 1.5\,\mathrm{km}$.

Figure 5 depicts effects of coherence length $\delta_g$ on effective beam sizes of the PCFPG beam when it propagates in turbulent atmosphere, with beam order $n = 2$ and $n = 4$, respectively. It can be found in these curves that PCFPG beams carrying smaller coherence length would have larger effective beam sizes upon propagation in turbulent atmosphere, and it can be compared to the spreading characteristics of some other partially coherent laser beams in turbulence [2, 7, 24, 29]. Illustrated figures also show that beams carrying larger order would have larger effective beam sizes upon propagation in turbulent atmosphere.

Figure 6 shows effects of atmospheric structure constant $C_n^2$ on effective beam sizes of PCFPG beams with order $n = 2$ and $n = 4$, respectively. It is found that, when $C_n^2$ increases, effective beam sizes

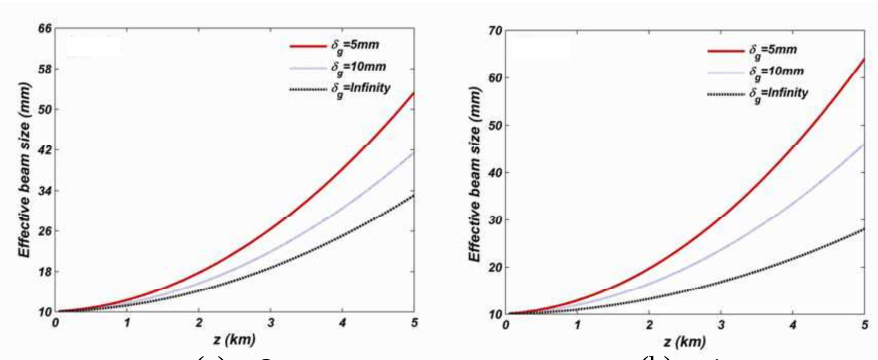


(a) n=2 (b) n=4

**Figure 5.** Effective beam sizes of PCFPG beams versus the propagation distance $z$ for different coherence length $\delta_g$ in turbulent atmosphere, $C_n^2 = 10^{-14}\,\mathrm{m}^{-2/3}$. (a) $n = 2$. (b) $n = 4$.

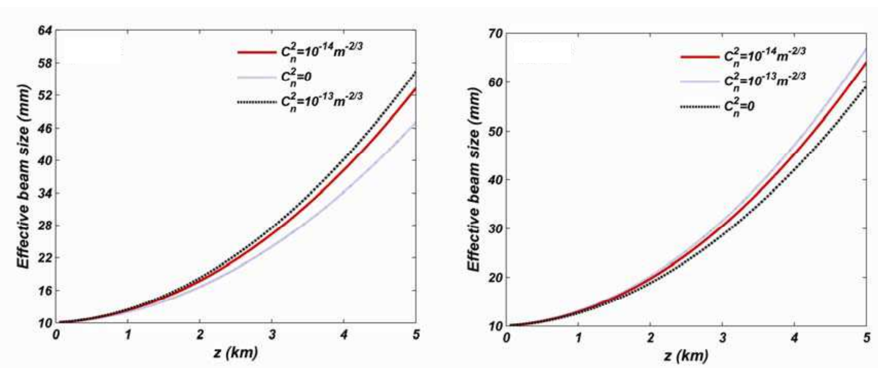


(a) n=2 (b) n=4

**Figure 6.** Effective beam sizes of PCFPG beams versus the propagation distance $z$ for different structure constant $C_n^2$ in turbulent atmosphere, $\delta_g = 5\,\mathrm{mm}$. (a) $n = 2$. (b) $n = 4$.

subsequently increase. By comparing Fig. 6(a) to Fig. 6(b), it also shows that higher-order PCFPG beams would be less affected by atmospheric turbulence than their lower order counterparts. Reasons of this phenomenon have been well explained in illustrations to Fig. 2.

Results obtained in this paper can be compared to some previous reports. Ref. [48] has revealed the propagation properties of the four-petal Gaussian beam with complete coherence through atmospheric turbulence. On the other hand, the four-petal Gaussian might be synthesized by utilizing coherent combinations of decentered Gaussian beams with the same initial phase [45, 46]. Based on this fact, for a practical synthesized four-petal Gaussian source beam, generally speaking, complete coherent case for such a laser beam can not be satisfied, in some sense. Therefore, the propositions of the PCFPG beam are essential to fields such as beam shaping and free space optical communications. Ref. [48] has reported the influence of turbulence on intensity distributions and spreading of the four-petal Gaussian beam when it propagates through atmosphere. Additionally, our paper not only considers effects of turbulent atmosphere, but also evaluates the influence of the coherence of sources on the propagation properties. These impacts are compositive, therefore deserved to be investigated. To the best our knowledge, these problem have not been referred in [45–52], even not reported so far. Phenomenons shown in Figs. 1–4 of our paper correspond well to the final conclusions of [10] that a general shaped laser beam will eventually approach to a Gaussian average intensity profile after it propagates in turbulent atmosphere. Furthermore, our results additionally demonstrate that, for the PCFPG beam propagating in atmosphere, the transformation of the intensity profile becomes much more rapidly when the coherence length $\delta_g$ decreases (see Fig. 4(d)).

## 4. CONCLUSIONS

In conclusion, intensity and beam spread of partially coherent four-petal Gaussian beam propagating in atmospheric turbulence is introduced in analytical forms. Based on the Huygens-Fresnel integral formula and mathematical treatments, average intensity distributions and effective beam sizes of PCFPG beams in turbulent atmosphere are derived in analytical expressions. Propagation properties of PCFPG beams in turbulence are investigated by numerical examples. It is indicated that the PCFPG beam deteriorates rapidly when it propagates in turbulent atmosphere, and it would convert into the Gauss-like profile sooner or later. It also shows that both source coherence length and atmospheric structure constant have essential influence on intensity distributions and effective beam sizes upon propagation. Results show that larger coherence length or higher beam order would lead to the reduction of degradations of PCFPG beams in turbulent atmosphere. These results may provide potential applications in free space optical communications and combination technology of high power laser beams.

## ACKNOWLEDGMENT

This work is supported by the National High Tech Research and Development Program of China (2007AA04Z181), the NUST Research Funding No. 2010ZYTS031 and the Excellent Doctorial Candidate Training Funding in NUST. Authors are indebted to the reviewers for their invaluable comments and suggestions.


## APPENDIX A. DERIVATIONS OF EQS. (7), (13) AND (14)

Equation (4) can be rewritten as the following form

$$W\left(x_1, y_1, x_2, y_2; 0\right) = \frac{[(2n)!]^4}{2^{12n}} \sum_{s=0}^{n}\sum_{t=0}^{n}\sum_{h=0}^{n}\sum_{l=0}^{n} \frac{1}{(n-s)!\,(2s)!\,(n-t)!\,(2t)!\,(n-h)!\,(2h)!\,(n-l)!\,(2l)!} \times H_{2s}\left(\frac{\sqrt{2}x_1}{\sigma_0}\right) H_{2t}\left(\frac{\sqrt{2}y_1}{\sigma_0}\right) H_{2h}\left(\frac{\sqrt{2}x_2}{\sigma_0}\right) H_{2l}\left(\frac{\sqrt{2}y_2}{\sigma_0}\right) \exp\left(-\frac{x_1^2+y_1^2+x_2^2+y_2^2}{\sigma_0^2}\right) \times \exp\left[-\frac{(x_1-x_2)^2+(y_1-y_2)^2}{2\delta_g^2}\right], \quad \text{(A1)}$$

Substituting Eq. (A1) and Eq. (6) into Eq. (5) and recalling the following equation [58]

$$\int_{-\infty}^{+\infty} \exp\left(-x^2+2xy\right) H_m(ax)\,dx = \exp\left(y^2\right)\sqrt{\pi}\left(1-a^2\right)^{\frac{m}{2}} H_m\left(\frac{ay}{\sqrt{1-a^2}}\right), \quad \text{(A2)}$$

After integrating over variables $x_1$, $y_1$, Eq. (5) can be arranged into the form

$$\langle I(p,q;z)\rangle = \frac{k^2}{4\pi z^2}\frac{[(2n)!]^4}{2^{12n}}\frac{1}{\sqrt{R_S^+R_S^-}}\exp\left(-\frac{k^2p^2}{4R_S^+z^2}-\frac{k^2q^2}{4R_S^+z^2}\right) \sum_{s=0}^{n}\sum_{t=0}^{n}\sum_{h=0}^{n}\sum_{l=0}^{n}\frac{\left(1-\frac{2}{R_S^+\sigma_0^2}\right)^{s+t}}{(n-s)!\,(2s)!\,(n-t)!\,(2t)!} \times\frac{1}{(n-h)!\,(2h)!\,(n-l)!\,(2l)!}$$

$$\int_{-\infty}^{+\infty}\exp\left\{-\left[R_S^- - \frac{\left(\frac{1}{\delta_g^2}+\frac{2}{\rho_0^2}\right)}{4R_S^+}\right]x_2^2+\frac{ikp}{z}\left[\frac{1}{2R_S^+}\left(\frac{1}{\delta_g^2}+\frac{2}{\rho_0^2}\right)-1\right]x_2\right\}$$

$$\times H_{2s}\left(\frac{\frac{1}{\delta_g^2}+\frac{2}{\rho_0^2}}{\sqrt{2{R_S^+}^2\sigma_0^2-4R_S^+}}x_2+\frac{ikp}{\sqrt{2{R_S^+}^2\sigma_0^2-4R_S^+z}}\right)H_{2h}\left(\frac{\sqrt{2}x_2}{\sigma_0}\right)dx_2$$

$$\times\int_{-\infty}^{+\infty}\exp\left\{-\left[R_S^- - \frac{\left(\frac{1}{\delta_g^2}+\frac{2}{\rho_0^2}\right)}{4R_S^+}\right]y_2^2+\frac{ikq}{z}\left[\frac{1}{2R_S^+}\left(\frac{1}{\delta_g^2}+\frac{2}{\rho_0^2}\right)-1\right]y_2\right\}$$

$$\times H_{2t}\left(\frac{\frac{1}{\delta_g^2}+\frac{2}{\rho_0^2}}{\sqrt{2{R_S^+}^2\sigma_0^2-4R_S^+}}y_2+\frac{ikq}{\sqrt{2{R_S^+}^2\sigma_0^2-4R_S^+z}}\right)H_{2l}\left(\frac{\sqrt{2}y_2}{\sigma_0}\right)dy_2, \quad \text{(A3)}$$

where $R_S^+$ has been given by Eq. (8) and $R_S^-$ in Eq. (A3) is represented by

$$R_S^- = \frac{1}{\sigma_0^2}+\frac{1}{2\delta_g^2}+\frac{1}{\rho_0^2}-\frac{ik}{2z}, \quad \text{(A4)}$$

Using the two following equations [58, 59]

$$H_m(x+y) = \frac{1}{2^{m/2}}\sum_{f=0}^{m}\binom{m}{f}H_f\left(\sqrt{2}x\right)H_{m-f}\left(\sqrt{2}y\right), \quad \text{(A5)}$$

$$H_f(x) = \sum_{u=0}^{[f/2]}(-1)^u\frac{f!}{u!\,(f-2u)!}(2x)^{f-2u}, \quad \text{(A6)}$$

Eq. (A3) can be further rewritten as

$$\langle I(p,q;z)\rangle = \frac{k^2}{4\pi z^2}\frac{[(2n)!]^4}{2^{12n}}\frac{1}{\sqrt{R_S^+R_S^-}}\exp\left(-\frac{k^2p^2}{4R_S^+z^2}-\frac{k^2q^2}{4R_S^+z^2}\right)$$

$$\sum_{s=0}^{n}\sum_{t=0}^{n}\sum_{h=0}^{n}\sum_{l=0}^{n}\frac{\left(\frac{1}{2}-\frac{1}{R_S^+\sigma_0^2}\right)^{s+t}}{(n-s)!\,(2s)!\,(n-t)!\,(2t)!}$$

$$\times\frac{1}{(n-h)!\,(2h)!\,(n-l)!\,(2l)!}\sum_{f=0}^{2s}\sum_{g=0}^{2t}\binom{2s}{f}\binom{2t}{g}$$

$$H_{2s-f}\left(\frac{ikp}{\sqrt{{R_S^+}^2\sigma_0^2-2R_S^+z}}\right)H_{2t-g}\left(\frac{ikq}{\sqrt{{R_S^+}^2\sigma_0^2-2R_S^+z}}\right)$$

$$\times \sum_{u=0}^{[f/2]} \sum_{v=0}^{h} \sum_{r=0}^{[g/2]} \sum_{d=0}^{2l} (-1)^{u+v+r+d}$$

$$\frac{f!\,(2h)!g!\,(2l)!}{u!\,(f-2u)!v!\,(2h-2v)!r!\,(g-2r)!d!\,(2l-2d)!} \left(\frac{8}{\sigma_0^2}\right)^{h+l-r-d}$$

$$\times \left(\frac{\frac{2}{\delta_g^2}+\frac{4}{\rho_0^2}}{\sqrt{{R_S^+}^2\sigma_0^2-2R_S^+}}\right)^{f+g-2u-2v} \int_{-\infty}^{+\infty} x_2^{f+2h-2u-2v}$$

$$\exp\left\{-R_Q^+ x_2^2 + \frac{ikp}{z}\left[\frac{1}{2R_S^+}\left(\frac{1}{\delta_g^2}+\frac{2}{\rho_0^2}\right)-1\right]x_2\right\} dx_2$$

$$\times \int_{-\infty}^{+\infty} y_2^{g+2l-2r-2d} \exp\left\{-R_Q^+ y_2^2 + \frac{ikq}{z}\left[\frac{1}{2R_S^+}\left(\frac{1}{\delta_g^2}+\frac{2}{\rho_0^2}\right)-1\right]y_2\right\} dy_2, \quad \text{(A7)}$$

where $R_Q^+$ also has been given by Eq. (8). Recalling the integral formula [58]

$$\int_{-\infty}^{+\infty} x^m \exp\left(-x^2+2\gamma x\right) dx = \exp\left(\gamma^2\right)(2i)^{-m}\sqrt{\pi}H_m(i\gamma), \quad \text{(A8)}$$

After integrating over variables $x_2$, $y_2$, Eq. (A7) would finally transform into Eq. (7). In order to derive expressions for effective beam sizes of PCFPG beams in turbulent atmosphere, by substituting Eqs. (4)–(6) into Eq. (11) and inverting the integration order, Recalling the formulas of the Dirac delta function $\delta$ [29, 60]

$$\delta^{(n)}(s) = \frac{1}{2\pi}\int_{-\infty}^{+\infty} (-ip)^n \exp(-isp)\, dp, \quad (n=0,1,2), \quad \text{(A9)}$$

$$\int_{-\infty}^{+\infty} f(x)\,\delta^{(n)}(x)\, dx = (-1)^n f^{(n)}(0), \quad (n=0,1,2), \quad \text{(A10)}$$

after tedious but straightforward integrations similar to procedures (A1)–(A7), we can finally obtain Eqs. (13) and (14).

## REFERENCES


1. Andrews, L. C. and R. L. Phillips, *Laser Beam Propagation Through Random Media*, SPIE Press, Bellingham, Washington, 1998.
2. Gbur, G. and E. Wolf, "Spreading of partially coherent beams in random media," *J. Opt. Soc. Am. A*, Vol. 19, 1592–1598, 2002.

3. Gbur, G. and R. K. Tyson, "Vortex beam propagation through atmospheric turbulence and topological charge conservation," *J. Opt. Soc. Am. A*, Vol. 25, 225–230, 2008.
4. Azana, J., "Lensless imaging of an arbitrary object," *Opt. Lett.*, Vol. 28, 501–503, 2003.
5. Ferri, F., D. Magatti, A. Gatti, M. Bache, E. Brambilla, and L. A. Lugiato, "High-resolution ghost image and ghost diffraction experiments with thermal light," *Phys. Rev. Lett.*, Vol. 94, 183602, 2005.
6. Cheng, J., "Ghost imaging through turbulent atmosphere," *Opt. Express*, Vol. 17, 7916–7921, 2009.
7. Ricklin, J. C. and F. M. Davidson, "Atmospheric turbulence effects on a partially coherent Gaussian beam: Implications for free-space laser communications," *J. Opt. Soc. Am. A*, Vol. 19, 1794–1802, 2002.
8. Chen, B., Z. Chen, and J. Pu, "Propagation of partially coherent Bessel-Gaussian beams in turbulent atmosphere," *Opt. Laser. Technol.*, Vol. 40, 820–827, 2008.
9. Qu, J., Y. Zhong, Z. Cui, and Y. Cai, "Elegant Laguerre-Gaussian beam in a turbulent atmosphere," *Opt. Commun.*, Vol. 283, 2772–2781, 2010.
10. Eyyuboglu, H. T., Y. Baykal, and E. Sermutlu, "Convergence of general beams into Gaussian intensity profiles after propagation in turbulent atmosphere," *Opt. Commun.*, Vol. 265, 399–405, 2006.
11. Ji, X., E. Zhang, and B. Lü, "Superimposed partially coherent beams propagating through atmospheric turbulence," *J. Opt. Soc. Am. B*, Vol. 25, 825–833, 2008.
12. Manez, R. J. and J. C. Gutiérrez, "Rytov theory for Helmholtz-Gauss beams in turbulent atmosphere," *Opt. Express*, Vol. 15, 16328–16341, 2007.
13. Razzaghi, D., F. Hajiesmaeilbaigi, and M. Alavinejad, "Turbulence induced changes in spectrum and time shape of fully coherent Gaussian pulses propagating in atmosphere," *Opt. Commun.*, Vol. 283, 2318–2323, 2010.
14. Eyyuboglu, H. T., Y. Baykal, and X. Ji, "Radius of curvature variations for annular, dark hollow and flat topped beams in turbulence," *Appl. Phys. B*, Vol. 99, No. 4, 801–807, 2010.
15. Shchepakina, E. and O. Korotkova, "Second-order statistics of stochastic electromagnetic beams propagating through non-Kolmogorov turbulence," *Opt. Express*, Vol. 18, 10650–10658, 2010.

16. Chen, W., J. W. Haus, and Q. Zhan, "Propagation of scalar and vector vortex beams through turbulent atmosphere," *Proc. of SPIE*, Vol. 7200, 720004, 2009.
17. Wang, F., Y. Cai, and O. Korotkova, "Partially coherent standard and elegant Laguerre-Gaussian beams of all orders," *Opt. Express*, Vol. 17, 22366–22379, 2009.
18. Shirai, T., A. Dogariu, and E. Wolf, "Directionality of Gaussian Schell-model beams propagating in atmospheric turbulence," *Opt. Lett.*, Vol. 28, 610–612, 2003.
19. Korotkova, O., M. Salem, and E. Wolf, "The far-zone behavior of the degree of polarization of electromagnetic beams propagating through atmospheric turbulence," *Opt. Commun.*, Vol. 233, 225–230, 2004.
20. Korotkova, O., "Control of the intensity fluctuations of random electromagnetic beam on propagation in weak turbulent atmosphere," *Proc. of SPIE*, Vol. 6105, 61050, 2006.
21. Cai, Y. and S. He, "Propagation of a partially coherent twisted anisotropic Gaussian Schell-model beam in turbulent atmosphere," *Appl. Phys. Lett.*, Vol. 89, 041117, 2006.
22. Arpali, C., C. Yazicioglu, H. T. Eyyuboglu, S. A. Arpali, and Y. Baykal, "Simulator for general-type beam propagation in turbulent atmosphere," *Opt. Express*, Vol. 14, 8918–8928, 2006.
23. Eyyuboglu, H. T., "Hermite-cosine-Gaussian laser beam and its propagation characteristics in turbulent atmosphere," *J. Opt. Soc. Am. A*, Vol. 22, 1527–1535, 2005.
24. Ji, X., X. Chen, and B. Lu, "Spreading and directionality of partially coherent Hermite-Gaussian beams propagating through atmospheric turbulence," *J. Opt. Soc. Am. A*, Vol. 25, 21–28, 2008.
25. Yuan, Y., Y. Cai, J. Qu, H. T. Eyyuboglu, and Y. Baykal, "Average intensity and spreading of an elegant Hermite-Gaussian beam in turbulent atmosphere," *Opt. Express*, Vol. 17, 11130–11139, 2009.
26. Li, J., Y. Chen, Q. Zhao, and M. Zhou, "Effect of astigmatism on states of polarization of aberrant stochastic electromagnetic beams in turbulent atmosphere," *J. Opt. Soc. Am. A*, Vol. 26, 2121–2127, 2009.
27. Chu, X., Z. Liu, and Y. Wu, "Propagation of a general multi-Gaussian beam in turbulent atmosphere in a slant path," *J. Opt. Soc. Am. A*, Vol. 25, 74–79, 2008.
28. Zhou, P., Z. Liu, X. Xu, and X. Chu, "Propagation of phase-locked

partially coherent flattened beam array in turbulent atmosphere," *Opt. & Laser. Eng.*, Vol. 47, 1254–1258, 2009.

29. Dan, Y. and B. Zhang, "Second moments of partially coherent beams in atmospheric turbulence," *Opt. Lett.*, Vol. 34, 563–565, 2009.
30. Zhou, G. and X. Chu, "Average intensity and spreading of a Lorentz-Gauss beam in turbulent atmosphere," *Opt. Express*, Vol. 18, 726–731, 2010.
31. Cai, Y., Y. Chen, H. T. Eyyuboglu, and Y. Baykal, "Scintillation index of elliptical Gaussian beam in turbulent atmosphere," *Opt. Lett.*, Vol. 32, 2405–2407, 2007.
32. Voelz, D. G. and X. Xiao, "Metric for optimizing spatially partially coherent beams for propagation through turbulence," *Opt. Eng.*, Vol. 48, 036001, 2009.
33. Gu, Y. and G. Gbur, "Measurement of atmospheric turbulences strength by vortex beam," *Opt. Commun.*, Vol. 283, 1209–1212, 2010.
34. Grynberg, G., A. Maitre, and A. Petrossian, "Flowerlike patterns generated by a laser beam transmitted through a rubidium cell with single feedback mirror," *Phys. Rev. Lett.*, Vol. 72, 2379–2382, 1994.
35. Zhang, B. and D. Zhao, "Focusing properties of Fresnel zone plates with spiral phase," *Opt. Express*, Vol. 18, 12818–12823, 2010.
36. Golub, I. and T. Mirtchev, "Absorption-free beam generated by a phase-engineered optical element," *Opt. Lett.*, Vol. 34, 1528–1530, 2009.
37. Pu, J., S. Nemoto, and X. Liu, "Beam shaping of focused partially coherent beams by use of the spatial coherence effect," *Appl. Opt.*, Vol. 43, 5281–5286, 2004.
38. Lindfors, K., T. Setälä, and M. Kaivola, "Degree of polarization in tightly focused optical fields," *J. Opt. Soc. Am. A*, Vol. 22, 561–568, 2005.
39. Zhan, Q. and J. R. Leger, "Focus shaping using cylindrical vector beams," *Opt. Express*, Vol. 10, 324–331, 2002.
40. Sabatke, D., A. Locke, E. L. Dereniak, M. Descour, J. Garcia, T. Hamilton, and R. W. McMillan, "Snapshot imaging spectropolarimeter," *Opt. Eng.*, Vol. 41, 1048–1054, 2002.
41. Ganic, D., X. Gan, and M. Gu, "Focusing of doughnut laser beams by a high numerical-aperture objective in free space," *Opt. Express*, Vol. 11, 2747–2752, 2003.
42. Wada, A., Y. Miyamoto, T. Ohtani, N. Nishihara, and M. Takeda,

"Effects of astigmatic aberration in holographic generation of Laguerre-Gaussian beam," *Proc. of SPIE*, Vol. 5137, 177–180, 2003.

43. Berre, M. L., A. S. Patrascu, E. Ressayre, and A. Tallet, "Daisy patterns in the passive ring cavity with diffusion effects," *Opt. Commun.*, Vol. 123, 810–824, 1996.
44. Firth, W. J., A. J. Scroggie, and G. S. Mcdonald, "Hexagonal patterns in optical bistability," *Phys. Rev. A*, Vol. 46, 3609–3612, 1992.
45. Cai, Y. and Q. Lin, "Four-beamlets laser array and its propagation," *Opt. Laser. Technol.*, Vol. 37, 483–489, 2005.
46. Duan, K. and B. Lu, "Four-petal Gaussian beams and their propagation," *Opt. Commun.*, Vol. 261, 327–331, 2006.
47. Gao, Z. and B. Lu, "Vectorial nonparaxial four-petal Gaussian beams and their propagation in free space," *Chin. Phys. Lett.*, Vol. 23, 2070–2073, 2006.
48. Chu, X., Z. Liu, and Y. Wu, "Propagation of four-petal Gaussian beams in turbulent atmosphere," *Chin. Phys. Lett.*, Vol. 25, 485–488, 2008.
49. Zhou, G. and Y. Fan, "$M^2$ factor of four-petal Gaussian beam," *Chin. Phys. B*, Vol. 17, 3708–3712, 2008.
50. Tang, B., Y. Jin, M. Jiang, and X. Jiang, "Diffraction properties of four-petal Gaussian beams in uniaxially anisotropic crystal," *Chin. Opt. Lett.*, Vol. 6, 779–781, 2008.
51. Tang, B., "Propagation properties of four-petal Gaussian beams in apertured factional Fourier transforming systems," *J. Mod. Opt.*, Vol. 56, 1860–1867, 2009.
52. Li, J., Y. Chen, Y. Xin, M. Zhou, and S. Xu, "Vectorial structural characteristics of four-petal Gaussian beams in the far field," *Eur. Phys. J. Appl. Phys.*, Vol. 50, 30702, 2010.
53. Mandel, L. and E. Wolf, *Optical Coherence and Quantum Optics*, Cambridge U. Press, 1995.
54. Wang, F., Y. Cai, H. T. Eyyuboglu, and Y. Baykal, "Average intensity and spreading of partially coherent standard and elegant Laguerre-Gaussian beams in turbulent atmosphere," *Progress In Electromagnetics Research*, Vol. 103, 33–56, 2010.
55. Li, J., Y. Chen, Y. Xin, M. Zhou, and S. Xu, "Diffraction properties of partially coherent vectorial four-petal Gaussian beams," *Opt. Commun.*, Vol. 283, 3105–3114, 2010.
56. Carter, W. H., "Spot size and divergence for Hermite-Gaussian beams of any order," *Appl. Opt.*, Vol. 19, 1027–1029, 1980.

57. Gbur, G. and E. Wolf, "The Rayleigh range of partially coherent beams," *Opt. Commun.*, Vol. 199, 295–304, 2001.
58. Gradshteyn, I. S. and I. M. Ryzhik, *Table of Integrals, Series, and Products*, Academic Press, New York, 1980.
59. Abramowitz, M. and I. Stegun, *Handbook of Mathematical Functions with Formulas, Graphs, and Mathematical Table*, U. S. Department of Commerce, 1970.
60. Bracewell, R. N., *The Fourier Transform and Its Applications*, 2nd edition, McGraw-Hill, 1986.